HAL
open science

Airborne measurements of HCl from the marine boundary layer to the lower stratosphere over the North Pacific Ocean during INTEX-B

S. Kim, L. G. Huey, R. E. Stickel, R. B. Pierce, G. Chen, M. A. Avery, J. E. Dibb, G. S. Diskin, G. W. Sachse, C. S. Mcnaughton, et al.

To cite this version:

S. Kim, L. G. Huey, R. E. Stickel, R. B. Pierce, G. Chen, et al.. Airborne measurements of HCl from the marine boundary layer to the lower stratosphere over the North Pacific Ocean during INTEX-B. Atmospheric Chemistry and Physics Discussions, 2008, 8 (1), pp.3563-3595. hal-00303983

HAL Id: hal-00303983

https://hal.science/hal-00303983v1

Submitted on 18 Jun 2008

HAL is a multi-disciplinary open access archive for the deposit and dissemination of scientific research documents, whether they are published or not. The documents may come from teaching and research institutions in France or abroad, or from public or private research centers.

L'archive ouverte pluridisciplinaire **HAL**, est destinée au dépôt et à la diffusion de documents scientifiques de niveau recherche, publiés ou non, émanant des établissements d'enseignement et de recherche français ou étrangers, des laboratoires publics ou privés.

Atmos. Chem. Phys. Discuss., 8, 3563–3595, 2008
www.atmos-chem-phys-discuss.net/8/3563/2008/
© Author(s) 2008. This work is distributed under
the Creative Commons Attribution 3.0 License.

Atmospheric Chemistry and Physics Discussions

Airborne measurements of HCl from the marine boundary layer to the lower stratosphere over the North Pacific Ocean during INTEX-B

S. Kim[1,6], L. G. Huey[1], R. E. Stickel[1], R. B. Pierce[2,7], G. Chen[2], M. A. Avery[2], J. E. Dibb[3], G. S. Diskin[2], G. W. Sachse[2,8], C. S. McNaughton[4], A. D. Clarke[4], B. E. Anderson[2], and D. R. Blake[5]

[1]School of Earth and Atmospheric Sciences, Georgia Institute of Technology, USA
[2]NASA Langley Research Center, USA
[3]Institute for the Study of Earth, Oceans, and Space, University of New Hampshire, USA
[4]Department of Oceanography, University of Hawaii, USA
[5]Department of Chemistry, University of California, Irvine, USA
[6]now at: Advanced Study Program, NCAR, Boulder CO, USA
[7]now at: NOAA/NESDIS Advanced Satellite Products Branch, Madison Wiv
[8]now at: National Institute of Aerospace, Hampton VA, USA

Received: 9 January 2008 – Accepted: 15 January 2008 – Published: 20 February 2008

Correspondence to: G. Huey (greg.huey@eas.gatech.edu)

Published by Copernicus Publications on behalf of the European Geosciences Union.

Abstract

Gas phase HCl was measured from the marine boundary layer (MBL) to the lower stratosphere from the NASA DC-8 during five science flights (41 h) of the Intercontinental Chemical Transport Experiment-Phase B (INTEX-B) field campaign. In the upper troposphere/lower stratosphere (UT/LS, 8–12 km) HCl was observed to range from a few tens to 100 pptv due to stratospheric influence with a background tropospheric level of less than 2 pptv. In the 8–12 km altitude range, a simple analysis of the O_3/HCl correlation shows that pure stratospheric and mixed tropospheric/stratospheric air masses were encountered 30% and 15% of the time, respectively. In the mid troposphere (4–8 km) HCl levels were usually below 2 pptv except for a few cases of stratospheric influence and were much lower than reported in previous work. These data indicate that background levels of HCl in the mid and upper troposphere are very low and confirm its use in these regions as a tracer of stratospheric ozone. However, a case study suggests that HCl may be produced in the mid troposphere by the dechlorination of dust aerosols. In the remote marine boundary layer HCl levels were consistently above 20 pptv (up to 140 pptv) and strongly correlated with HNO_3. Cl atom levels were estimated from the background level of HCl in the MBL. This analysis suggests a Cl concentration of $\sim 3\times10^3$ atoms cm^{-3}, which corresponds to the lower range of previous studies. Finally, the observed HCl levels are compared to predictions by the Real-time Air Quality Modeling System (RAQMS) to assess its ability to characterize the impact of stratospheric transport on the upper troposphere.

1 Introduction

Hydrochloric acid (HCl) is produced in the troposphere and stratosphere by different mechanisms. In the troposphere the major source of HCl is thought to be dechlorination of sea-salt aerosol by acids such as HNO_3 and H_2SO_4 (Erickson, 1959a, b; Kerminen et al., 1998). HCl is very soluble in water and can be lost to cloud drops and aerosols

ACPD

8, 3563–3595, 2008

of non-acidic composition (Keene et al., 1999) on the time scale of a day in the remote marine boundary layer (MBL). Conversely, the lifetime of HCl with respect to photolysis and reaction with OH is relatively long (~20 days with $[OH]_{AVG}=10^6$ molecules cm^{-3}) in the troposphere (Sander et al., 2006). For this reason, tropospheric HCl chemistry is expected to be most active in the MBL. This is especially true in the polluted MBL where very high levels of HCl have been predicted (~400 pptv; Spicer et al., 1998). These high levels have been attributed to the interaction of N_2O_5 with sea-salt, which can produce Cl_2 (Behnke et al., 1997; Schweitzer et al., 1998; Rossi, 2003). Cl_2 will be rapidly photolyzed to produce chlorine atoms that produce HCl by reaction with methane and other volatile organic compounds (VOC). Elevated Cl_2 in the urban MBL has been suggested to lead to enhanced ozone production (Finley and Saltzman, 2006; Tanaka et al, 2003; Chang et al., 2002; Spicer et al., 1998).

Direct observations of HCl in the MBL and lower troposphere are limited in terms of frequency and geographical coverage. However, HCl has been measured in a variety of locations (Graedel and Keene, 1995). These measurements indicate HCl mixing ratios in the remote MBL (0–200 m) of 100–300 pptv with levels decreasing to 50–100 pptv in the remote marine free troposphere (1 km–6 km; Vierkorn-Rudolph et al., 1984). In the urban influenced troposphere, ppbv levels of HCl have been reported in various locations (Keene et al., 2007; Graedel and Keene, 1995). Keene et al. (1999) calculated the global tropospheric budget of HCl, based on the data from Graedel and Keene (1995), and reported that additional sources are needed to explain the distribution of HCl in the troposphere. However, this conclusion was based on data from analytical methods (filter techniques), which have been identified to potentially have positive artifacts such as NOCl, $ClNO_2$, $ClNO_3$ and chlorinated aerosols. Therefore, most of these studies report HCl*, which includes these and potentially other species.

The magnitude of HCl production in the troposphere by Cl reactions with VOC is not well constrained due to the uncertainty in Cl levels. A series of studies have applied indirect methods using chemical proxies such as observations of C_2Cl_4 and VOC ratios to estimate Cl number densities (Singh et al., 1996a, 1996b; Wingenter et al., 1996, 1999,

2005; Rudolph et al., 1996, 1997; Jobson et al., 1998; Arsene et al., 2007). These estimates range from 720 atoms cm^{-3} (Wingenter et al., 1999) to 10^5 atoms cm^{-3}(Singh et al., 1996a; Wingenter et al., 1996).

In the stratosphere HCl is produced primarily by the reaction of Cl radicals with CH_4 (Lin et al., 1978). The source of stratospheric chlorine is the photodissociation of chlorofluorocarbons (CFCs) (Molina and Rowland, 1974). HCl is the most abundant form of inorganic chlorine in the stratosphere due to its long photochemical lifetime (~30 days at 20 km, Webster et al., 1994). However, HCl can be lost via heterogeneous processes in the stratosphere (Hanson et al., 1994; Hanson and Ravishakara, 1991, 1993, and 1994; Tolbert et al., 1988). Lelieveld et al. (1999) reported a mean mixing ratio of ~450 pptv of HCl at 12.3 km in the late Arctic winter (Feburary 1995; Kiruna, Sweden) from observations with a quadrupole mass spectrometer. Webster et al. (1994) also reported in situ HCl measurements in the stratosphere using a tunable diode laser spectrometer integrated on the NASA ER-2 research aircraft during the Stratospheric Photochemistry, Aerosols, and Dynamics Expedition (SPADE) mission. These research flights covered a latitude range of 15–60° N and altitudes below 20 km in spring and fall of 1992 and 1993. HCl levels of 500 pptv to 1ppbv of HCl were observed over a pressure range of 50 to 70 mb. In addition, this study also found that model predictions of the HCl fraction of inorganic chlorine (Cl_y=HCl, ClO, and $ClONO_2$) in the stratosphere were systematically higher than observations although the model predicted Cl_y within the uncertainty of the measurement.

Remote sensing has been used to measure the global distribution of HCl in the stratosphere. The Halogen Occultation Experiment (HALOE) indicated ~1 ppbv of HCl at 10 mb with no obvious variation as a function of season or latitude (Russell et al., 1996).

Recently, Marcy et al. (2004) demonstrated the utility of HCl measurements for examining the transport of stratospheric O_3 to the troposphere. They found a very high degree of correlation between HCl and O_3 in the upper troposphere and lower stratosphere during the Cirrus Regional Study of Tropical Anvils and Cirrus Layers-Florida

Area Cirrus Experiment (CRYSTAL-FACE) mission. They also found the observed relationship to be consistent with the Integrated Massively Parallel Atmospheric Chemistry Transport (IMPACT) model of stratospheric chemistry (Rotman et al., 2004). Consequently, they proposed using the observed HCl-O_3 ratio to calculate the fraction of stratospheric ozone in an air parcel. However, this method relies on the assumption that HCl in the free troposphere is only of stratospheric origin which is inconsistent with previous observations (e.g. Graedel and Keene, 1995).

In this work we present observations of HCl from the NASA DC-8 during the Anchorage, AK deployment of the Intercontinental Chemical Transport Experiment-Phase B (INTEX-B). This phase of the mission consisted of five flights over the North Pacific as shown in Fig. 1. Each science mission consisted of level flight legs and multiple spiral vertical profiles from the MBL to the upper troposphere (UT). The comprehensive vertical coverage allows us to examine HCl levels over the entire troposphere. These data are analyzed using correlations with other measured species and a 3-D chemical transport model to probe our understanding of the sources and distribution of HCl in the troposphere.

2 Methods

2.1 Instrumentation

The chemical ionization mass spectrometer (CIMS) integrated on the NASA-DC 8 aircraft for the INTEX-B campaign was identical to that used in INTEX-North America (NA) and is described in detail in Kim et al. (2007) and Slusher et al. (2004). The instrument comprises an inlet, a flow tube ion molecular reactor, a collisional dissociation chamber (CDC), an octopole ion guide, and a quadrupole mass filter. SF_6^- ion chemistry is utilized to selectively ionize HCl and SO_2 (R1 and R2) in the CIMS flow tube reactor (Huey, 2007; Slusher et al., 2001; Huey et al., 1995).

$$HCl + SF_6^- \rightarrow SF_5Cl^- + HF \qquad \text{(R1a)}$$

ACPD
8, 3563–3595, 2008

$$HCl + SF_6^- \rightarrow Cl^-(HF) + SF_5 \quad \text{(R1b)}$$

$$HCl + SF_6^- \rightarrow SF_5^- + ? \quad \text{(R1c)}$$

$$SO_2 + SF_6^- \rightarrow F_2SO_2^- + SF_4 \quad \text{(R1d)}$$

R1a was chosen to detect HCl, as it has the highest yield (~45%), is more selective than R1c, and was less prone to interference than R1b. The sensitivity of the CIMS to HCl was not calibrated during the science flight. The sensitivity to SO_2 was periodically measured (every 2.5 min) by standard additions of $^{34}SO_2$ to the inlet (R2). Periodic background checks to both SO_2 and HCl were performed using an activated charcoal and nylon wool scrubber (~every 10 min). The temporal variations of the HCl and SO_2 product ions during a science flight are presented in Fig. 2.

The sensitivity of HCl relative to SO_2 was assessed post mission by a series of laboratory tests over the pressure and the humidity conditions encountered on the DC-8. These experiments demonstrate that the sensitivity ratio of HCl and SO_2 is a strong function of water vapor (Fig. 3) at dewpoints below −15°C. The sensitivity to SO_2 has a negative correlation with humidity due to the hydrolysis of the product ion $F_2SO_2^-$. However, the sensitivity to HCl was found to be essentially independent of humidity. For this reason, the HCl sensitivity at dewpoints below −15°C was calculated relative to the SO_2 standard addition. However, at dewpoints above −15°C, the strong correlation between the sensitivity of HCl and the reagent ion signal ($^{34}SF_6^-$) was utilized to obtain the HCl sensitivity. An estimated uncertainty of 33% was obtained from considering potential errors in the gas standards (SO_2, 5% and HCl, 10%), the dew point measurement (5%) and the post-mission calibrations (18%) combined with the statistical error at the 2σ level of the in flight calibration (1 s average, 25%). The lower limit of detection (LLOD) for HCl was estimated to be 2 pptv for a signal to noise ratio of one with the noise defined as 2σ of the background signal for a 30 s average.

In earlier work we have pointed out that ozone and in particular water vapor are potential interferences for detection of any ambient species using CIMS and SF_6^- ion

chemistry (Slusher et al., 2001). For this reason, the selectivity of the HCl measurement was further assessed by taking in-flight mass spectra in both the stratosphere (high O_3) and the MBL (high water vapor) (Fig. 4). These results showed low background levels in the region of the product ion (162 amu) and exhibit the expected isotope signature of SF_5Cl^-(^{35}Cl: ^{37}Cl). These results indicate that the HCl measurement at SF_5Cl^- is viable over a wide range of atmospheric conditions. These observations were also confirmed with laboratory tests that demonstrated that SF_5Cl^- detection channel is essentially immune to interference from water vapor and ozone. However, the product channel Cl^-(HF), R1b, has significant interferences due to water vapor at even moderate dew points.

2.2 Model

We compare measured HCl levels and HCl:O_3 correlations with model predictions by the Real-time Air Quality Modeling System (RAQMS), which was developed for the prediction of both tropospheric and stratospheric chemistry and assimilation of satellite based atmospheric composition measurements (Pierce et al., 2003; Pierce et al., 2007). A retrospective 9-month (February–October 2006) 2×2 degree ozone and carbon monoxide chemical analysis, including assimilation of cloud cleared Ozone Monitoring Instrument (OMI) total column ozone measurements and ozone and carbon monoxide profiles from Tropospheric Emission Spectrometer (TES) nadir measurements from the NASA Aura satellite was conducted to support INTEX-B post mission analysis. Retrievals from daily TES global survey mode observations between 60° S and 60° N were assimilated. The assimilation accounts for the trace gas retrieval sensitivities by convolving the model first guess ozone profile with the OMI and TES averaging kernels and a priories. Since the TES L2 quality flags have been developed primarily for tropospheric retrievals we restricted assimilation of TES CO to below the local tropopause while TES O_3 was assimilated below 10 mb. The RAQMS HCl predictions were not constrained with observations. The RAQMS meteorological forecasts are initialized from NOAA Global Forecasting System (GFS) analyses at 6-hour intervals.

3 Results and discussion

All reported data and analyses are based on a 1 min merged dataset unless otherwise noted. The median and the mean attitude profiles of HCl for five science flights of the INTEX-B mission are presented in Fig. 5, along with the median profiles of O_3 and HNO_3. In addition, in Table 1, we report the statistics of the vertical distribution of HCl. In general, we found high HCl episodes (up to 140 pptv) in the upper troposphere (8–12 km) interspersed with observations of low levels near our detection limit of 2 pptv. Although the median value of the highest altitude bin in the figure indicates a low value, it should be noted that this value represents only 10 min of data from one flight leg. In the MBL, HCl levels above 20 pptv were routinely observed. In the mid troposphere (4–8 km), HCl was measured below 15 pptv more than 90% of the time. However, one case of strong stratospheric influence was identified by HCl enhancement along with enhanced O_3. There was also evidence for one episode of dechlorination in the mid troposphere. The vertical distribution of HCl in this study is significantly different from that of Keene et al. (1999) and Graedel and Keene (1995). The observed values in both the MBL and mid troposphere are lower by a factor of 5–10 than the previous studies. This may indicate that other species besides HCl are the major contributors to HCl* observations in the mid troposphere. The observations of very low background levels of HCl in the UT are consistent with the results reported by Marcy et al. (2004).

3.1 The upper troposphere (8–12 km)

High levels of HCl in the upper troposphere were strongly associated with stratospheric influences. This is illustrated in Fig. 6a and b, which show a strong negative correlation of HCl with tropospheric tracers (N_2O and CFCs), and Fig. 6c and d which show a strong positive correlation of HCl with stratospheric tracers (O_3 and HNO_3). The correlation with O_3 (Fig. 6c) illustrates that the background level of HCl (i.e. w/o stratospheric influence) in the upper troposphere is low and that HCl is a good tracer for recent stratospheric influence. HCl also shows a strong positive (R^2=0.77) correlation

with Be-7, another stratospheric tracer measured on the DC-8 with a 15 min integration time (Dibb et al., 2003).

The method of Marcy et al. (2004) was employed to assess the extent of stratospheric influence on the upper troposphere during the Anchorage deployment of INTEX-B. This method utilizes the O_3-HCl correlation (Fig. 7a) and sets a stratospheric end member (O_3: 160 ppbv and HCl: 30 pptv). Above the end member the air is categorized as pure stratospheric. Air parcels with HCl below detection limit are categorized as pure tropospheric air. In between these limits the air is characterized as a mixture of both. The analysis suggests that in the upper troposphere (8–12 km) during INTEX-B pure stratospheric air was sampled ~30% of the time and air with significant stratospheric influence (i.e. detectable HCl) was observed ~15% of the time.

Figure 7a also contains the predicted correlation of HCl with O_3 by the RAQMS model in the upper troposphere. The modeled slope (0.33) overestimates the observed slope (0.22) by 50%, slightly larger than the estimated measurement error. Marcy et al. (2004) found better agreement between their observed HCl-O_3 ratio and IMPACT model results during two CRYSTAL-FACE flights. Marcy et al. (2004) reported significantly higher observed ratios (0.44 and 0.51) of HCl/O_3 than in this work (0.22). This higher ratio may be due to the CRYSTAL-FACE study being conducted in the summer in the subtropics (24° N–39° N) at a higher altitude range (11–18 km). However, both measurement model comparisons of the HCl to ozone slope indicate that there is a well understood relationship between stratospheric HCl and O_3.

Figure 7b presents a strong correlation (R^2=0.72) between measured and RAQMS predicted HCl in the upper troposphere. However, the linear regression has a slope of ~0.5 with a significant offset (17 pptv), which indicates underestimation of HCl at higher concentrations (>35 pptv) by RAQMS. Therefore, the overestimated HCl/O_3 ratio from RAQMS may reflect discrepancies between the RAQMS analyzed and measured O_3 rather than HCl. Comparisons between the RAQMS ozone analysis and O_3 measurements from the Anchorage DC8 flights indicate that the RAQMS OMI+TES analysis underestimates lower stratospheric ozone (>120 ppbv) by a factor of 2, which

accounts for much of the HCl/O_3 discrepancies. The positive offset in the modeled HCl suggests that the RAQMS model either over predicts stratosphere-troposphere exchange or under predicts wet scavenging of HCl since no other source of chlorine is available in the model. Finally, the upper tropospheric data set of RAQMS is classified with the scheme of Marcy et al. (2004) with corrected end-members of stratospheric influenced air (O_3>120 ppbv) and pure tropospheric air (HCl<17 pptv). The results predict a higher fraction than observations for stratospheric influenced air (~44%) and underestimate the amount of pure tropospheric air (~20%) suggesting that RAQMS overestimates stratosphere-troposphere exchange processes. However, in general the RAQMS model appears to do a reasonable job of capturing the broader features of stratospheric impact on the upper troposphere given the relatively coarse horizontal resolution (2×2 degree) of the analysis.

3.2 The MBL and the Lower Troposphere (0–4 km)

The median levels of HCl (Fig. 5 and Table 1) increase at altitudes below 4 km and reach up to 20 pptv in the MBL (z<1 km). These observations are much lower than recent measurements in the relatively clean Hawaii MBL of 30–250 pptv (Pszenny et al., 2004). Figure 8a and b shows the correlation of HCl with SO_2 and HNO_3 in the MBL (z<1 km), respectively. Both species show a good correlation with HCl except for a few outliers associated with either volcanic influence, from the Veniaminof volcano, located in the Aleutian Island chain, or anthropogenic pollution near the western U.S. coast. These positive correlations with HNO_3 and SO_2, the major precursor of H_2SO_4, are consistent with HCl production from the acidification of sea-salt aerosol (assuming that HCl has a relatively short lifetime in the MBL).

However, at very low levels of HNO_3 and SO_2, significant levels of HCl were still observed (~20 pptv). These low levels of HCl in the absence of HNO_3 and SO_2 could be produced by the reactions of Cl atoms with VOCs. This is supported by enhanced *i*-butane/*n*-butane ratios (median=0.7), which is consistent with Cl atom oxidation (Jobson et al., 1994). A simple calculation to estimate the number density of Cl atoms

needed to produce this amount of HCl is conducted using the assumption that HCl is in steady state. Three HCl loss pathways: aerosol uptake, oceanic deposition, and reaction with OH, are considered. Lifetimes for each loss process are estimated based on the INTEX-B data summarized in Table 2. These assumptions give the equation below for calculation of the Cl atom number density.

$$[Cl] = \frac{[HCl] \times (k_{OH} + k_{Dry-Deposition} + k_{Aerosol-Uptake})}{k_1[Ethane] + k_2[Propane] + k_{34}[Ethyne] + k_4[Methane] + k_5[DMS]} \quad (1)$$

The input parameters (Table 2) are based on observations from the INTEX dataset and rate constants from the JPL compilation (Sander et al., 2006). A dry deposition rate of 1.6 cm s^{-1} is estimated based upon Kerkweg et al. (2006). An accommodation coefficient of 0.15 is used to calculate HCl loss to aerosol (Sander et al., 2006). The average result of the calculation is 2.8×10^3 atoms cm^{-3}. Probably the most uncertain of these parameters is the dry deposition rate of HCl. Dry deposition rates are expected to range from 0.2–2.0 cm s^{-1} over a water surface (Seinfeld and Pandis, 2006). This indicates the derived value is probably an upper limit to the Cl atom number density as the dry deposition rate is only likely to be slower. The derived estimate (2.8×10^3 atoms cm^{-3}) is in the lower range (Singh et al., 1996b; Rudolph et al., 1996, 1997; Jobson et al., 1998; Wingenter et al., 1999) of previous studies and is not compatible with higher estimates of greater than 10^5 atom cm^{-3} (Singh et al., 1996a; Wingenter et al., 1996). The most recent reports of Cl atom levels are toward the higher end of the range; 6×10^3–4.7×10^4 atoms cm^{-3} by Arsene et al. (2007) and 5.7×10^4 atoms cm^{-3} by Wingenter et al. (2005). The levels are significantly larger than in this work but are derived for tropical locations and may not be directly comparable to our results.

During the INTEX-B campaign, most boundary layer legs were conducted in unpolluted regions. However, one flight in the MBL south of Seattle, WA did intercept moderate levels of pollution (Fig. 9). Consequently, enhancements of HCl might be expected due to both dechlorination and NO_x activated processes as suggested by a series of

studies (e.g. Spicer et al., 1997) and recent observations (Keene et al., 2007). Large enhancements of HCl were not observed in the polluted air mass (09:02 to 09:05 PM in the Fig. 9). However, the sampling duration was very short (~3 min) and was over a limited geographic area, though.

3.3 The mid troposphere (4–8 km)

Figure 10 presents the correlation between O_3 and HCl in the mid-troposphere (4–8 km). Although HCl levels in the mid-troposphere were usually low (<2 pptv 55%, and <15 pptv 90%), significant levels of HCl were observed that were associated with stratospheric influence and had a similar ratio of O_3 to HCl as at higher altitudes (~7.5 km). However, Fig. 10 also shows that HCl enhancements (more than 20 pptv) can be observed with no stratospheric influence (i.e. no enhancement in O_3 and incompatible back trajectories). To investigate the origin of the non-stratospheric HCl in the mid troposphere we examined two aircraft spirals in similar geographical locations with contrasting HCl. These profiles are shown in Fig. 11 with spiral 1 having undetectable HCl and spiral 2 with significant HCl in the mid troposphere.

The transport of HCl to the mid troposphere from the MBL could explain the enhancement in spiral 2. However, RAQMS backtrajectory analyses show that this air mass had resided in the mid troposphere for ~5 days without any influence from either the stratosphere or the MBL. Moreover, chemical tracers such as O_3 for the stratosphere, and CH_3I and CH_3NO_3 for the MBL were not enhanced in the mid troposphere during spiral 2. In fact they are very similar levels to those observed in the non-enhanced spiral 1. In addition, ambient temperature profiles demonstrate that the mid troposphere during both spiral 1 and spiral 2 was stratified (Fig. 12). Consequently, we are skeptical that the HCl in the mid troposphere has a recent MBL origin. However, there are high levels of non-volatile aerosol (T>350°C) in the mid troposphere that correspond with enhanced scattering at 450 nm in spiral 2 (Fig. 12). The properties of the nonvolatile aerosol (e.g. the ratio of refractory aerosol to total aerosols and the aerosol depolarization) all indicate that it is primarily dust of Asian origin. There is evidence from

recent field studies that dust particles can absorb significant amounts of chlorine when passing through the MBL (Sullivan et al., 2007; Ooki and Uematsu, 2005; Zhang and Iwasaka, 2001). This dust could undergo dechlorination later by exposure to strong acids such as nitric and sulfuric. High levels of HNO_3 and SO_2 are observed in spiral two that are consistent with the air mass having been in contact with urban areas such as Shanghai, China as indicated by a 7-day back trajectory analysis in Fig. 11b). For these reasons, we speculate that the mid-tropospheric HCl in this case is produced by dechlorination of dust particles activated by the oxidation of anthropogenic pollution. It is doubtful if this mechanism is a large source of HCl to the atmosphere. However, this mechanism should be recognized as a potential interference to using HCl as a stratospheric tracer in the free troposphere. In addition, the production of HCl from dust particles provides a mechanism to transform the chemical composition of the dust aerosol.

4 Summary

Airborne measurements of HCl during the Anchorage deployment of the INTEX-B field mission provide a unique dataset from the MBL to the lower stratosphere over the North Pacific Ocean. In the upper troposphere (z>8 km), HCl serves as a good tracer for recent stratospheric influence due to its very low background concentration (less than 2 pptv) and it well defined relationship with stratospheric ozone. A simple analysis using the HCl/O_3 correlation illustrates that ~50% of the air above 8 km (up to 12 km) was either stratospheric (~30%) or recent stratospheric influenced air (~15%). The RAQMS model systematically overestimated the HCl/O_3 correlation by 50%. In addition, RAQMS underestimated observed HCl by ~30% at higher levels (>60 pptv) although both measured and model predicted HCl show a strong correlation (R^2=0.74) in the upper troposphere. These results demonstrate the ability of RAQMS to broadly predict the impact of stratospheric mixing on the upper troposphere.

In the remote MBL HCl levels were consistently above 20 pptv (up to 105 pptv)

and strongly correlated with HNO_3. This is consistent with dechlorination of sea-salt aerosols by gas phase acids as the major source of HCl in the MBL. One sampling leg (~15 min) in a polluted coastal boundary layer (south of Seattle, WA) did not show significant enhancements of HCl relative to the remote MBL which is in contrast with other studies. The background level of HCl in the MBL was used to estimate average Cl atom number density of 3×10^3 atoms/cm^3, which is consistent with the lower range of previous studies.

In the mid troposphere (4–8 km), HCl was usually below our detection limit of 2 pptv, which is consistent with recent in situ measurement of HCl in the upper troposphere by Marcy et al. (2004). On a few occasions HCl associated with enhanced O_3 was detected due to recent stratospheric influences. In addition, enhanced HCl not of stratospheric origin was detected in the mid troposphere. This HCl appears to have been produced by dechlorination of Asian dust aerosols.

The measured HCl profiles in this work indicate above the MBL that background tropospheric levels of HCl are very low (<2 pptv). This is consistent with the findings of Marcy et al. (2004) but is inconsistent with the profile of Keene et al. (1999). However, profiles obtained in this study are over a limited geographic region (Northern Pacific Ocean) which may be a reason for the disagreement. Consequently, observations by the method presented in this paper over a wider geographic range would be useful to sort out this difference.

Acknowledgements. This work was supported by NASA Tropospheric Chemistry Program (Contract # NNG06GA78G). We thank the flight crew of the NASA DC-8. LGH is grateful to D. W. Fahey for very useful discussions of this work. The view, opinions, and findings contained in this report are those of the author(s) and should not be construed as an official National Oceanic and Atmospheric Administration or U.S. Government position, policy, or decision.

References

Arsene, C., Bougiatioti, A., Kanakidou, M., Bonsang, B., and Mihalopoulos, N.: Tropospheric OH and Cl levels deduced from non-methane hydrocarbon measurements in a marine site, Atmos. Chem. Phys., 7, 4661–4673, 2007, http://www.atmos-chem-phys.net/7/4661/2007/.

Behnke, W., George, C., Scheer, V., and Zetzsch, C.: Production and decay of $ClNO_2$ from the reaction of gaseous N_2O_5 with NaCl solution: Bulk and aerosol experiments, J. Geophys. Res., 102, 3795–3804, 1997.

Chang, S., McDonald-Buller, E. C., Kimura, Y., Yarwood, G., Neece, J. D., Russell, M., Tanaka, P., and Allen, D.: Sensitivity of urban ozone formation to chlorine emission estimates, Atmos. Environ., 36, 4991–5003, 2002.

Dibb, J. E., Talbot, R. W., Scheuer, E., Seid, G., and DeBell, L.: Stratospheric influence on the northern North American free troposphere during TOPSE: ^{7}Be as a stratospheric tracer, J. Geophys. Res., 108, 8368, doi:8310.1029/2001JD001347, 2003.

Erickson, E.: The yearly circulation of chloride and sulfur in nature; meteorological, geochemical and pedological implications, Part I., Tellus, 11, 375–403, 1959.

Erickson, E.: The yearly circulation of chloride and sulfur in nature; meteorological, geochemical and pedological implications, Part II., Tellus, 12, 63–109, 1959.

Finley, B. and Saltzman, E.: Measurement of Cl_2 in coastal urban air, Geophys. Res. Lett., 33, L11809, doi:11810.11029/12006GL025799, 2006.

Graedel, T. E. and Keene, W. C.: Tropospheric budget of reactive chlorine, Glob. Biogeochem. Cy., 9, 47–77, 1995.

Hanson, D. R. and Ravishankara, A. R.: The reaction probabilities of $CONO_2$ and N_2O_5 on 40 to 75% sulfuric acid solutions, J. Geophys. Res., 96, 17 307–17 314, 1991.

Hanson, D. R. and Ravishankara, A. R.: Reaction of $CLONO_2$ with HCl on NAT, NAD, and frozen sulfuric acid and hydrolysis of N_2O_5 and $ClONO_2$ on frozen sulfuric acid, J. Geophys. Res., 98, 22 931–22 936, 1993.

Hanson, D. R. and Ravishankara, A. R.: Reactive uptake of $ClONO_2$ onto sulfuric acid due to reaction with HCl and H_2O, J. Phys. Chem., 98, 5728–5735, 1994.

Hanson, D. R., Ravishankara, A. R., and Solomon, S.: Heterogeneos reactions in sulfuric acid aerosols: A framework for model calculations, J. Geophys. Res., 99, 3615–3629, 1994.

Huey, L. G.: Measurement of trace atmospheric species by chemical ionization mass spec-

trometry: Speciation of reactive nitrogen and future directions, Mass Spectrom. Rev., 26, 166–184, 2007.
Huey, L. G., Hanson, D. R., and Howard, C. J.: Reactions of SF_6^- and I^- with atmospheric trace gases, J. Phys. Chem., 99, 5001–5008, 1995.
Jobson, B. T., Niki, H., Yokouchi, Y., Bottenheim, J., Hopper, F., and Leaitch, R.: Measurements of C2–C6 hydrocarbons during the Polar Sunrise 1992 Experiment: Evidence for Cl atom and Br atom chemistry, J. Geophy. Res., 99, D12, 25 355–25 368, 1994.
Jobson, B. T., Parrish, D., Goldan, P., Kuster, W., Feshenfeld, F. C., Blake, D. R., Blake, N. J., and Niki, H.: Spatial and temporal variability of nonmethane hydrocarbon mixing ratios and their relation to photochemical lifetime, J. Geophys. Res., 103, 13 557–13 567, 1998.
Keene, W. C., Aslam, M., Khalil, K., Erickson, D. J., McCulloch, A., Graedel, T. E., Lobert, J. M., Aucott, M. L., Gong, S. L., Harper, D. B., Kleiman, G., Midgley, P., Moore, R. M., Seuzaret, C., Sturges, W. T., Benkovitz, C. M., Koropalov, V., Barrie, L. A., and Li, Y. F.: Composite global emissions of reactive chlorine from anthropogenic and natural resorces; Reactive Chlorine Emissions Inventory, J. Geophys. Res., 104, 8429–8440, 1999.
Keene, W. C., Stutz, J., Pszenny, A. P., Maben, J. R., Fischer, E. V., Smith, A. M., von Glasow, R., Pechtl, S., Sive, B. C., and Varner, R. K.: Inorganic chlorine and bromine in coastal New England air during summer, J. Geophys. Res., 112, doi:10.1029/2006JD007689, 2004.
Kerminen, V.-M., Teinila, K., Hillamo, R., and Pakkanen, T.: Substitution of chloride in sea-salt paticles by inorganic and organic anions, J. Aerosol Sci., 29, 929–942, 1998.
Kim, S., Huey, L. G., Stickel, R. E., Tanner, D. J., Crawford, J. H., Olson, J. R., Chen, G., Brune, W. H., Ren, X., Lesher, R., Wooldridge, P. J., Bertram, T. H., Perring, A., Cohen, R. C., Lefer, B. L., Shetter, R. E., Avery, M., Diskin, G., and Sokolik, I.: Measurement of HO_2NO_2 in the free troposphere during the Intercontinental Chemical Transport Experiment-North America 2004, J. Geophys. Res., 112, D12S01, doi:10.1029/2006JD007676, 2007.
Kerkweg, A., Buchholz J., Ganzeveld L., Pozzer, A., Tost H., and Jökel, P.: Technical Note: An implementation of the dry removal processes DRY DEPosition and SEDImentation in the Modular Earth Submodel System (MESSy), Atmos. Chem. Phys., 6, 4617–4632, 2006, http://www.atmos-chem-phys.net/6/4617/2006/.
Lelieveld, J., Bregman, A., Scheeren, H. A., Strom, J., Carslaw, K. S., Fischer, H., Siegmund, P. C., and Arnold, F.: Chlorine activation and ozone destruction in the northern lowermost stratosphere, J. Geophys. Res., 104, 8201–8212, 1999.
Lin, C. L., Leu, M. T., and DeMore, W. B.: Rate constant for the reaction of atomic chlorine with

methane, J. Phys. Chem., 82, 1772–1777, 1978.
Marcy, T. P., Fahey, D. W., Gao, R. S., Popp, P. J., Richard, E. C., Thompson, T. L., Rossenlof, K. H., Ray, E. A., Salawitch, R. J., Atherton, C. S., Bergmann, D. J., Ridley, B. A., Weinheimer, A. J., Loewenstein, M., Weinstock, E. M., and Mahoney, M. J.: Quantifying stratospheric ozone in the upper troposphere with in situ measurements of HCl, Science, 304, 261–265, 2004.
Molina, M. J. and Rowland, F. S.: Stratospheric sink for chlorofluoromethanes:Chlorine-atom catalysed destruction of ozone, Nature, 249, 810–812, 1974.
Ooki, A., and Uematsu, M.: Chemical interactions between mineral dust particles and acid gases during Asian dust events, J. Geophys. Res., 110, D03201, doi:10.1029/2004JD004737, 2005.
Pierce, R. B., Al-Saadi, J. A., Schaack, T., Lenzen, A., Zapotocny, T., Johnson, D. G., Kittaka, C., Buker, M., Hitchman, M. H., Tripoli, G., Fairlie, T. D., Olson, J. R., Natarajan, M., Crawford, J., Fishman, J., Avery, M., Browell, E., Creilson, J., Kondo, Y., and Sandholm, S. T.: Regional Air Quality Modeling System (RAQMS) predictions of the tropospheric ozone budget over east Asia, J. Geophys. Res., 108, 8825, doi:8810.1029/2002JD003176, 2003.
Pierce, R. B., Schaack, T., Al-Saadi, J. A., Fairlie, T. D., Kittaka, C., Lingenfelser, G., Natarajan, M., Olson, J., Soja, A., Zapotocny, T., Lenzen, A., Stobie, J., Johnson, D., Avery, M. A., Sachse, G. W., Thompson, A., Cohen, R., Dibb, J. E., Crawford, J., Rault, D., Martin, R., Szykman, J.,and Fishman, J.: Chemical data assimilation estimates of continental U.S. ozone and nitrogen budgets during the Intercontinental Chemical Transport Experiment-North America, J. Geophys. Res. 112, D12S21, doi:10.1029/2006JD007722, 2007.
Pszenny, A. A. P., Moldanova, J., Keene, W. C., Sander, R., Maben, J. R., Martinez, M., Crutzen, P. J., Perner, D., and Prinn, R. G.: Halogen cycling and aerosol pH in the Hawaiian marine boundary layer, Atmos. Chem. Phys., 4, 147–168, 2004, http://www.atmos-chem-phys.net/4/147/2004/.
Rossi, M. J.: Heterogeneous reactions on salts, Chemical Reviews, 103, 4823–4882, 2003.
Rotman, D. A., Atherton, C. S., Bergmann, D. J., Cameron-Smith, P. J., Chuang, C. C., Connell, P. S., Dignon, J. E., Franz, A., Grant, K. E., Kinnison, D. E., Molenkamp, C. R., Proctor, D. D., and Tannahill, J. R.: IMPACT, the LLNL 3-D global atmospheric chemical transport model for the combined troposphere and stratosphere: Model description and analysis of ozone and other trace gases, J. Geophys. Res. 109, D04303, doi:10.1029/2002JD003155, 2004.
Rudolph, J., Koppmann, R., and Plass-Dulmer, C.: The budget of ethane and tetra-

chloroethene: Is there evidence for an impact of reactions with chlorine atoms in the troposphere?, Atmos. Environ., 30, 1887–1894, 1996.
Rudolph, J., Ramacher, B., Plass-Dulmer, C., Muller, K.-P., and Koppmann, R.: The indirect determination of chlorine atom concentration in the troposhere from changes in the patterns of non-methane hydrocarbons, Tellus, 49B, 592–601, 1997.
Russell III, J. M., Deaver, L. E., Luo, M., Park, J. H., Gordley, L. L., Tuck, A. F., Toon, G. C., Gunson, M. R., Traub, W. A., Johnson, D. G., Jucks, K. W., Murcray, D. G., Zander, R., Nolt, I. G., and Webster, C. R.: Validation of hydrogen chloride measurements made by the Halogen Occultation Experiment from the UARS platform, J. Geophys. Res., 101, 10 151–10 162, 1996.
Sander, S. P., Friedl, R. R., Ravishankara, A. R., Golden, D. M., Kolb, C. E., Kurylo, M. J., Molina, M. J., Mootgat, G. K., Finlayson-Pitts, B. J., Wine, P. H., Huie, R. E., and Orkin, V. L.: Chemical kinetics and photochemical data for use in atmospheric studies, Evaluation Number 15, JPL Publication 06–2, 2006.
Schweitzer, F., Mirabel, P., and George, C.: Multiphase chemistry of N_2O_5, $ClNO_2$ and $BrNO_2$, J. Phys. Chem. A, 102, 3942–3952, 1998.
Seinfeld J. H. and Pandis S. N.: Atmospheric Chemistry and Physics: From Air Pollution to Climate Change, Wiley-Interscience, 2nd edition, New York, 2006.
Singh, H. B., Gregory, G. L., Anderson, B., Browell, E., Sachse, G. W., Davis, D. D., Crawford, J., Bradshaw, J. D., Talbot, R., Blake, D. R., Thornton, D., Newell, R., and Merrill, J.: Low ozone in the marine boundary layer of the tropical pacific ocean;Photochemical loss, chlorine atoms, and entrainment, J. Geophys. Res., 101, 1907–1914, 1996a.
Singh, H. B., Thakur, A. N., Chen, Y. E., and Kanakidou, M.: Tetrachloroethylene as an indicator of low Cl atom concentrations in the troposphere, Geophys. Res. Lett., 23, 1529–1532, 1996b.
Slusher, D. L., Huey, L. G., Tanner, D. J., Flocke, F., and Roberts, J. M.: A thermal dissociation-chemical ionization mass spectrometry (TD-CIMS) technique for the simultaneous measurement of peroxyacyl nitrates and dinitrogen pentaoxide, J. Geophys. Res., 109(D19), D19315, doi:10.1029/2004JD004670, 2004.
Slusher, D. L., Pitteri, S. J., Haman, B. J., Tanner, D. J., and Huey, L. G.: A chemical ionization technique for measurement of pernitric acid in the upper troposphere and the polar boundary layer, Geophys. Res. Lett., 28, 3875–3878, 2001.
Spicer, C. W., Chapman, E. G., Finlayson-Pitts, B. J., Plastridege, R. A., Hubbe, J. M., and

Fast, J. D.: Unexpected high concentrations of molecular chlorine in coastal air, Nature, 394, 353–356, 1997.
Sullivan, R. C., Guazzotti, S. A., Sodeman, D. A., and Prather, K. A.: Direct observations of the atmospheric processing of Asian mineral dust, Atmos. Chem. Phys., 7, 1213–1236, 2007, http://www.atmos-chem-phys.net/7/1213/2007/.
Tanaka, P. L., Riemer, D. D., Chang, S., Yarwood, G., McDonald-Buller, E. C., Apel, E. C., Orlando, J. J., Silva, P. J., Jimenez, J. L., Canagaratna, M. R., Neece, J. D., Mullins, C. B., and Allen, D. T.: Direct evidence for chlorine-enhanced urban ozone formation in Houston, Texas, Atmos. Environ., 37, 1393–1400, 2003.
Tolbert, M. A., Rossi, M. J., and Golden, D. M.: Heterogeneous interactions of chlorine nitrate hydrogen chloride and nitric acid with sulfuric acid surfaces at stratospheric temperatures, Geophys. Res. Lett., 15, 847–850, 1988.
Vierkorn-Rudolph, B., Bachmann, K., Schwarz, B., and Meixner, F. X.: Vertical profiles of hydrogen chloride in the troposphere, J. Atmos. Chem., 2, 47–63, 1984.
Webster, C. R., May, R. D., Jaegle, L., Hu, H., Sander, S. P., Gunson, M. R., Toon, G. C., Russell III, J. M., Stimpfle, R. M., Koplow, J. P., Salawitch, R. J., and Michelsen, H. A.: Hydrochloric acid and the chlorine budget of the lower stratosphere, Geophys. Res. Lett., 21, 2575–2578, 1994.
Wingenter, O. W., Sive, B. C., Blake, N. J., Blake, D. R., and Rowland, F. S.: Atomic chlorine concentration derived from ethane and hydroxyl measurements over the equatorial Pacific Ocean: Implication for dimethyl sulfide and bromine monoxide, J. Geophys. Res., 110, D20308, doi:10.1029/2005JD005875, 2005.
Wingenter, O. W., Blake, D. R., Blake, N. J., Sive, C., Rowland, F. S., Atlas, E., and Flocke, F.: Tropospheric hydroxyl and atomic chlorine concentrations, and mixing timescales determined from hydrocarbon and halocarbon measurements mad over the Southern Ocean, J. Geophys. Res., 104, 21 819–21 818, 1999.
Wingenter, O. W., Kubo, M. K., Blake, N. J., Smith, J., T. W., Blake, D. R., and Rowland, F. S.: Hydrocarbon and halocarbon measurements as photochemical and dynamical indicators of atmospheric hydroxyl, atomic chlorine, and vertical mixing obtained during Lagrangian flights, J. Geophys. Res., 101, 4331–4340, 1996.
Zhang, D., and Iwasaka, Y.: Chlorine deposition on dust particles in marine atmosphere, Geophys. Res. Lett., 28, 3613–3616, 2001.

Table 1. Vertical distribution of one minute averaged HCl mixing ratios (pptv) from five science flights during the Anchorage deployment of the INTEX-B campaign.

Altitude	Average	Median	1σ	Min.	Max.
0.25	32.1	24.4	20.9	5.8	105.1
0.75	22.8	17.5	18.0	8.1	82.6
1.25	18.3	14.1	17.0	2.0	72.0
1.75	16.9	11.2	14.6	2.0	72.2
2.25	18.0	13.8	14.0	2.0	80.7
2.75	8.3	6.3	12.6	2.0	64.8
3.25	7.4	8.6	5.8	2.0	29.3
3.75	6.9	5.8	6.5	2.0	28.2
4.25	5.5	2.0	5.8	2.0	25.2
4.75	6.1	2.0	6.1	2.0	25.5
5.25	6.0	2.0	7.1	2.0	24.1
5.75	6.8	6.7	6.0	2.0	23.5
6.25	4.4	2.0	4.5	2.0	22.0
6.75	5.0	2.0	5.8	2.0	20.7
7.25	8.1	2.0	11.4	2.0	56.0
7.75	5.9	2.0	8.7	2.0	55.0
8.25	9.8	2.0	13.6	2.0	55.2
8.75	27.7	14.2	33.5	2.0	115.4
9.25	6.6	2.0	11.0	2.0	55.9
9.75	26.2	2.0	31.8	2.0	89.4
10.25	54.5	62.3	43.5	2.0	140.9
10.75	1.23	2.0	1.7	2.0	7.0

Table 2. Summary of input parameters for the calculation of average Cl atom number densities.

Species	Concentrations	k_{Cl} (molecules^{-1}cm^3 s^{-1})
Ethane	1.5 ppbv	5.58×10^{-11}
Propane	242 pptv	1.40×10^{-10}
Ethyne	257 pptv	5.81×10^{-11}
Methane	1.86 ppmv	7.01×10^{-14}
DMS	7 pptv	1.93×10^{-10}
Loss Pathways		Rates
k_{OH}		0.048 day^{-1}
$k_{Aerosol_Uptake}$		2.0 day^{-1}
$k_{Dry_Deposition}$		2.0 day^{-1}

ACPD
8, 3563–3595, 2008

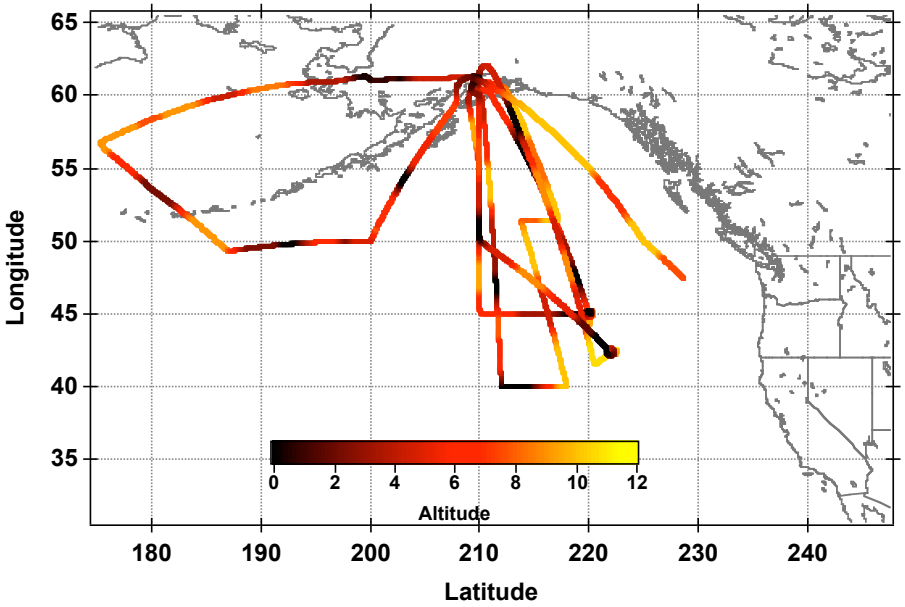

Fig. 1. Flight tracks color coded by altitude during the Anchorage deployment of the INTEX campaign.

ACPD
8, 3563–3595, 2008

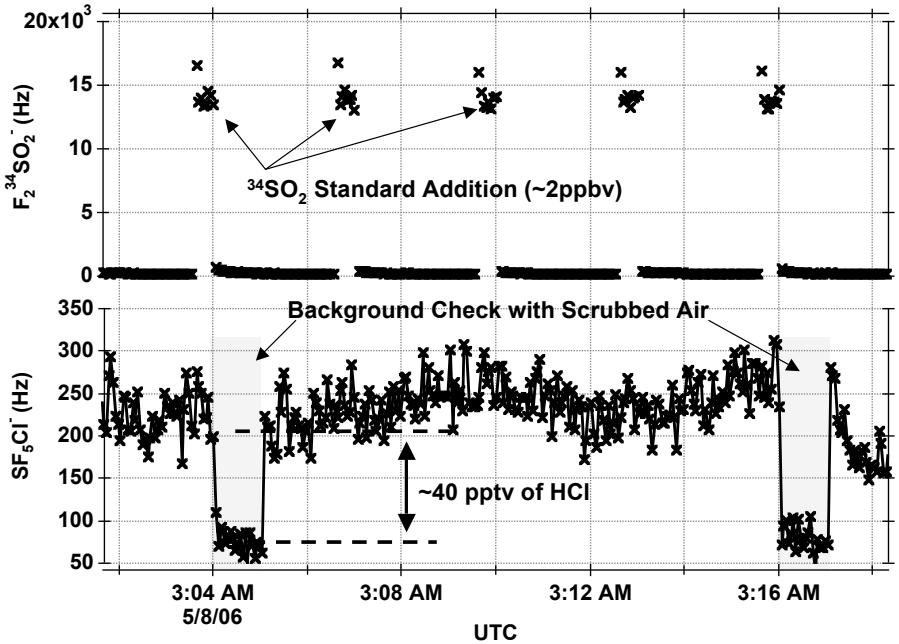

Fig. 2. Typical temporal variations of the $^{34}SO_2$ calibration signal (the upper panel) and the ambient HCl signal (the lower panel) during the science flight. Note that the noise on the HCl background on the 0.5 s measurement points is less than +/−8 pptv.

ACPD
8, 3563–3595, 2008

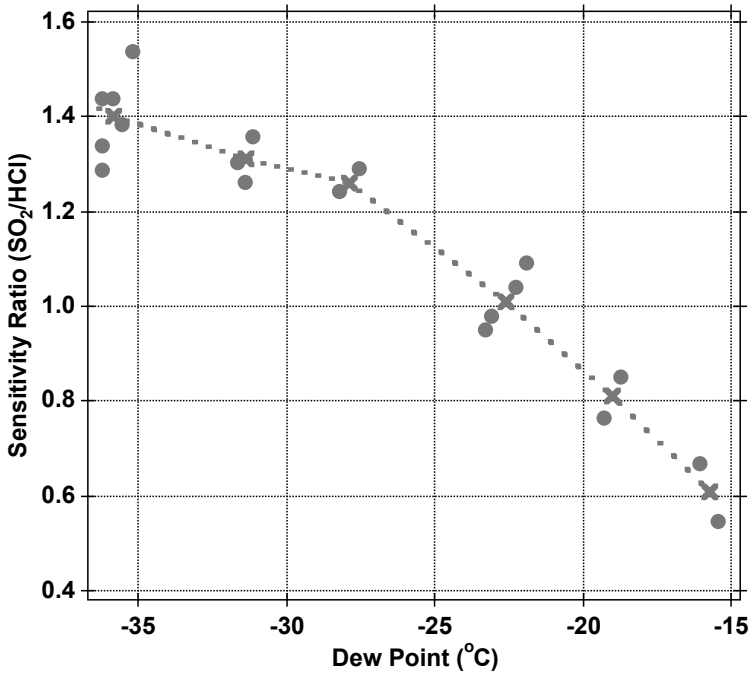

Fig. 3. The sensitivity ratio of HCl/SO_2 as a function of dew point.

ACPD
8, 3563–3595, 2008

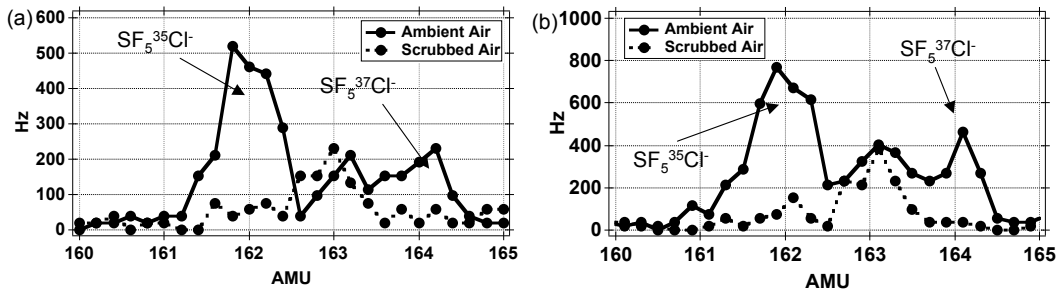

Fig. 4. Mass spectra obtained in **(a)** stratospheric air with high O_3 and **(b)** the MBL with high water vapor. Each data point is a 0.5 s integration.

ACPD
8, 3563–3595, 2008

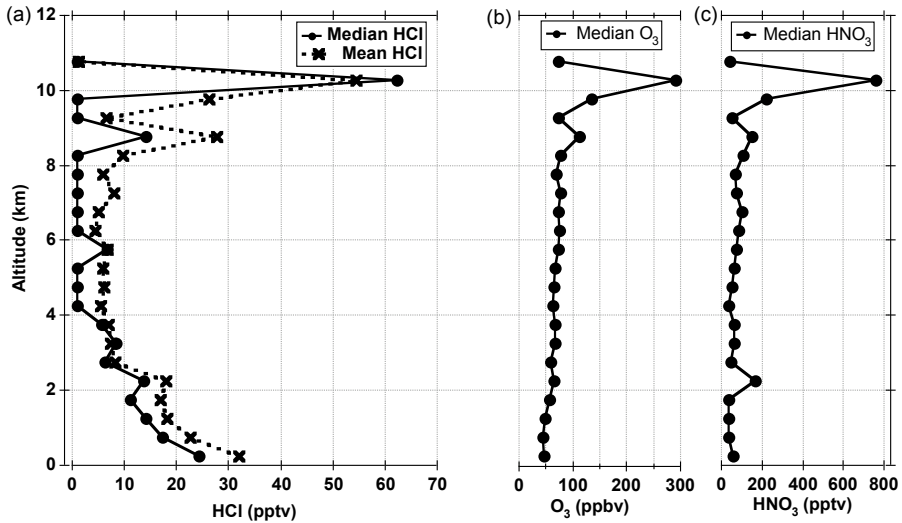

Fig. 5. The median and mean altitude profile of HCl and the median profiles of O_3 and HNO_3.

ACPD
8, 3563–3595, 2008

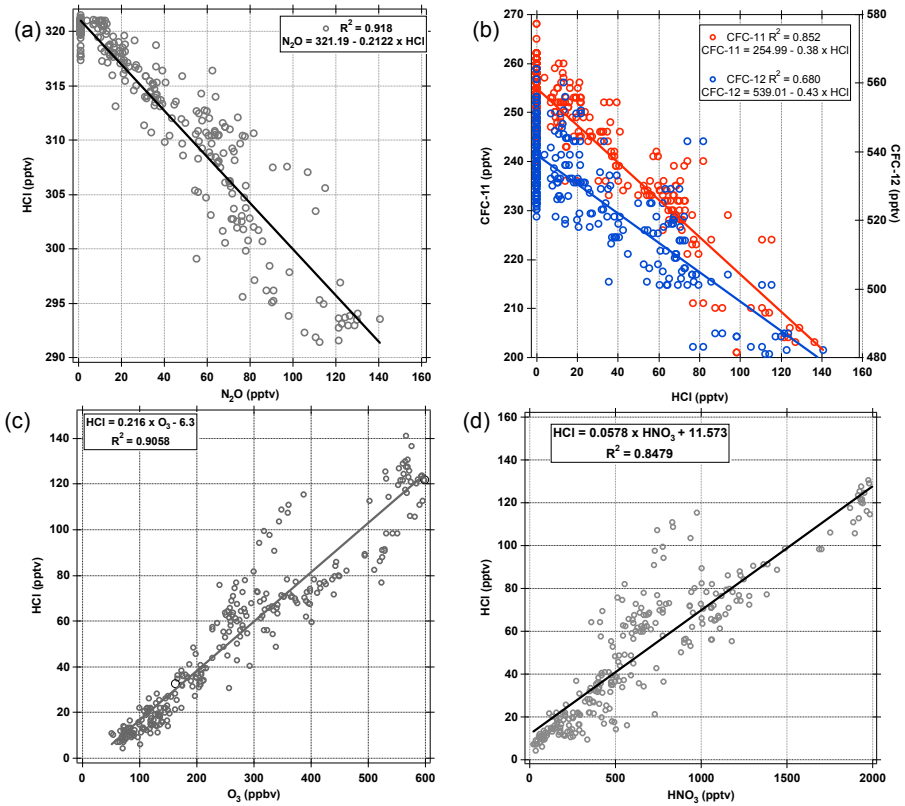

Fig. 6. The correlation of HCl with **(a)** N_2O, **(b)** CFCs **(c)** O_3, and **(d)** HNO_3 in the upper troposphere (8–12 km).

ACPD
8, 3563–3595, 2008

HCl from the marine boundary layer to the lower stratosphere

S. Kim et al.

CC BY

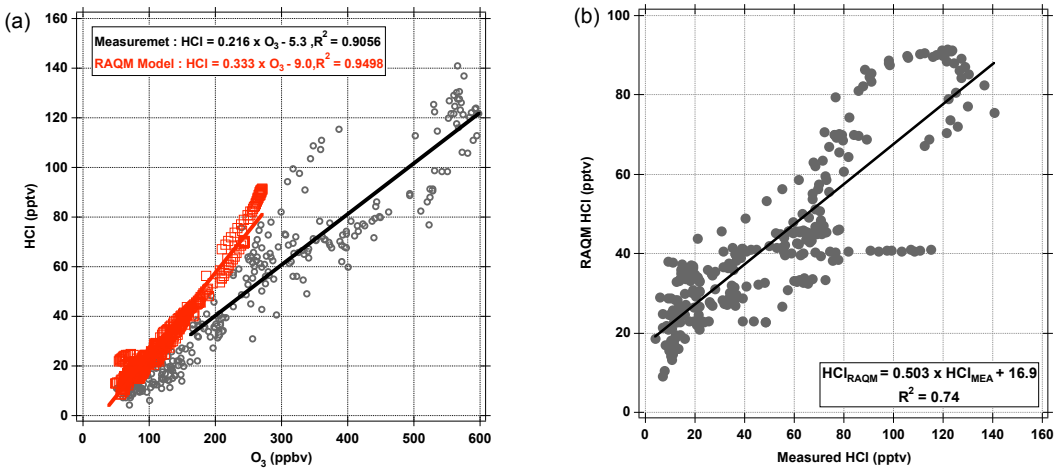

Fig. 7. The correlation of HCl with O_3 in the upper troposphere from in situ measurements (black open circles) and RAQMS model results (red open squares). Regression lines of each result are also presented. **(b)** Correlation plot between measured and RAQMS predicted HCl.

ACPD
8, 3563–3595, 2008

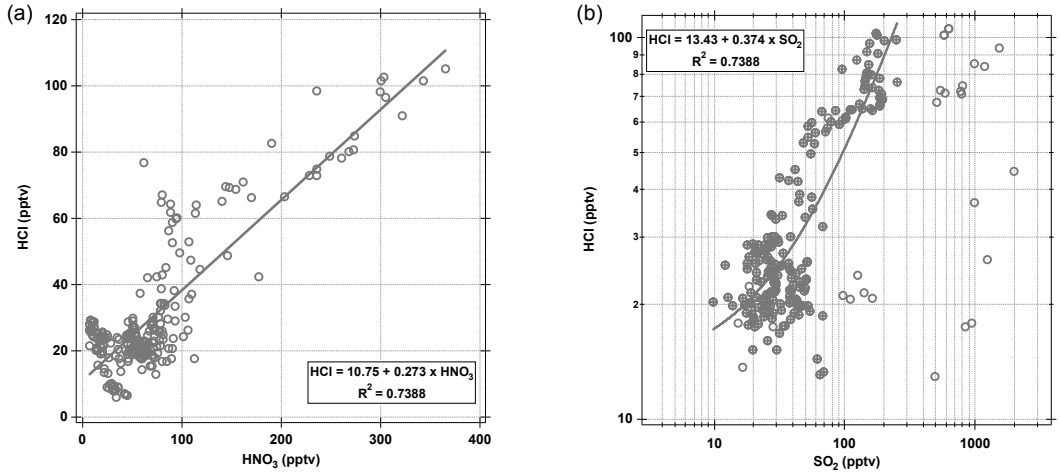

Fig. 8. Correlation plots of marine boundary layer HCl with **(a)** HNO_3 and **(b)** SO_2.

ACPD
8, 3563–3595, 2008

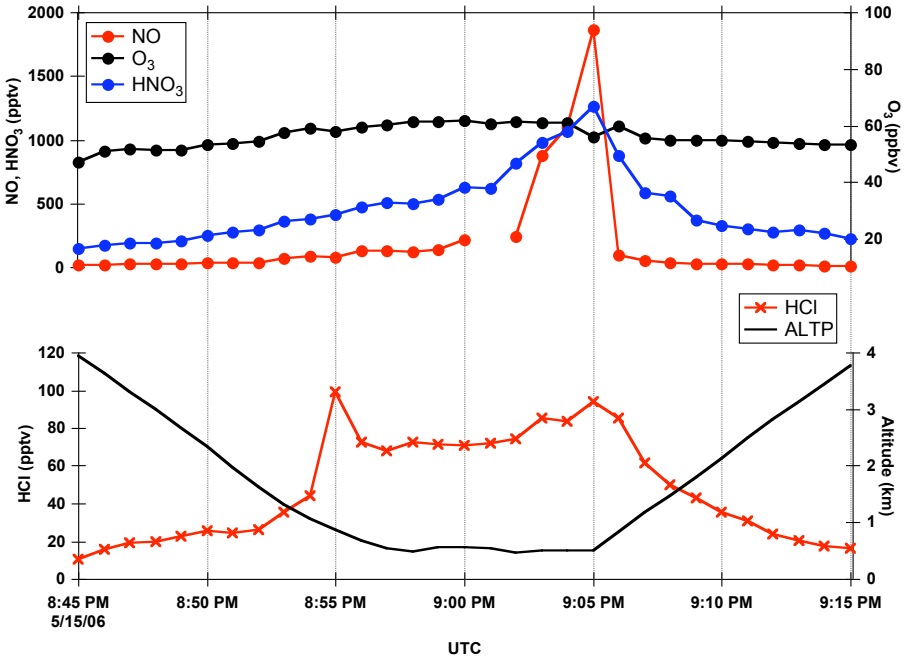

Fig. 9. Temporal variations of HCl, O_3, NO, and altitude during coastal boundary layer sampling near Seattle, WA. No obvious enhancement of HCl was detected in this high NO_x environment.

ACPD
8, 3563–3595, 2008

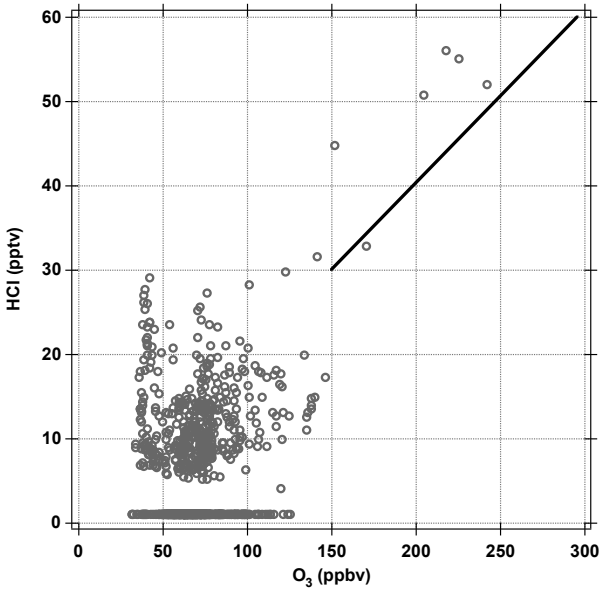

Fig. 10. The correlation of HCl with O_3 in the mid troposphere (4–8 km). The line represents the HCl-O_3 regression line of the stratosphere in Fig. 7.

ACPD
8, 3563–3595, 2008

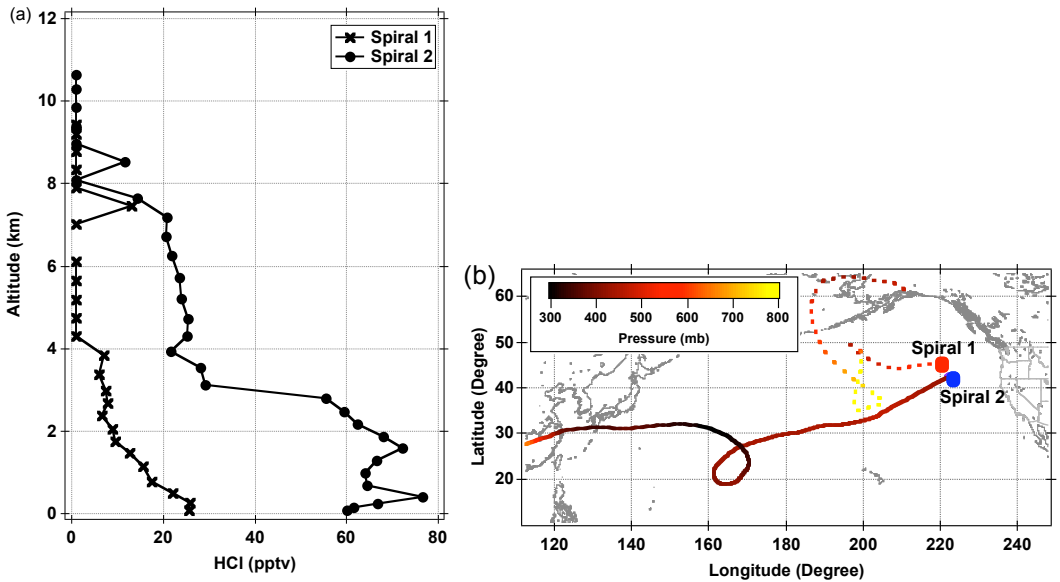

Fig. 11. (a) HCl profiles from two different aircraft spirals (spiral 1–x, spiral 2–•). **(b)** Seven day back trajectories for both spirals.

ACPD
8, 3563–3595, 2008

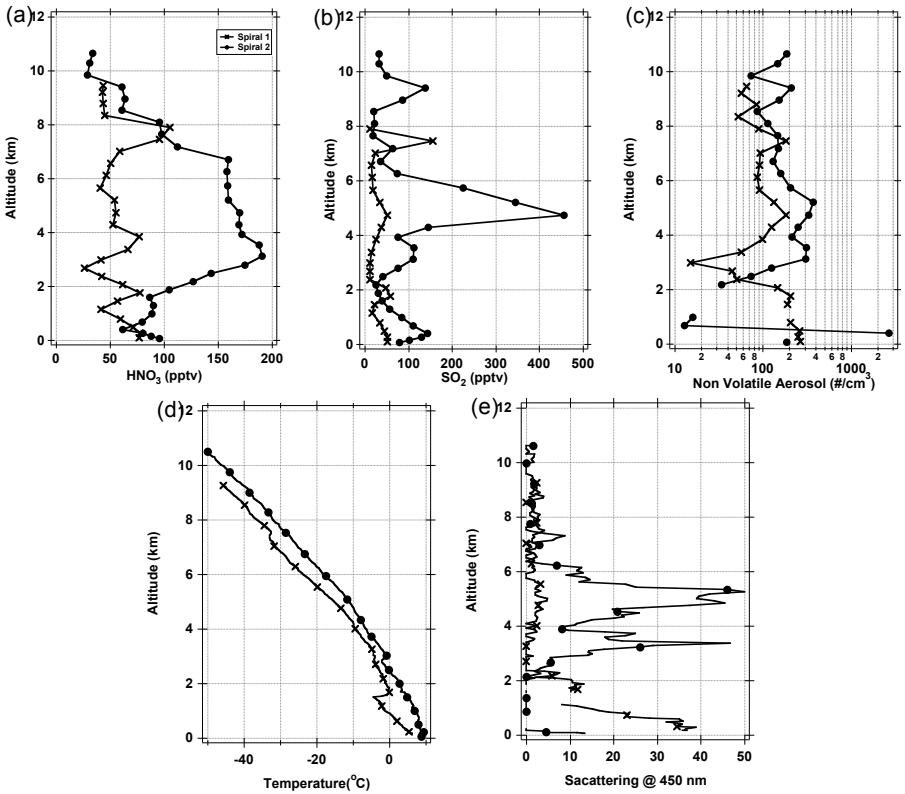

Fig. 12. Vertical profiles of **(a)** HNO_3, **(b)** SO_2, **(c)** non volatile aerosols. **(d)** temperature, and **(e)** aerosol scattering at 450 nm. (spiral 1–x, spiral 2–•).

ACPD
8, 3563–3595, 2008